









RESEARCH ARTICLE | AUGUST 21 2023

Mean flow modeling in high-order nonlinear Schrödinger equations

Alexis Gomel ; Corentin Montessuit ; Andrea Armaroli ; Debbie Eeltink ; Amin Chabchoub ; Jérôme Kasparian ; Maura Brunetti  

 Check for updates

Physics of Fluids 35, 087128 (2023)

<https://doi.org/10.1063/5.0164784>



View Online



Export Citation

CrossMark

AIP Advances

Why Publish With Us?



25 DAYS
average time
to 1st decision



740+ DOWNLOADS
average per article



INCLUSIVE
scope

[Learn More](#)



AIP
Publishing

Mean flow modeling in high-order nonlinear Schrödinger equations

Cite as: Phys. Fluids **35**, 087128 (2023); doi: [10.1063/5.0164784](https://doi.org/10.1063/5.0164784)

Submitted: 24 June 2023 · Accepted: 5 August 2023 ·

Published Online: 21 August 2023



View Online



Export Citation



CrossMark

Alexis Gomel,^{1,a)}  Corentin Montessuit,¹  Andrea Armaroli,^{1,b)}  Debbie Eeltink,^{2,3,4}  Amin Chabchoub,^{5,6} 
Jérôme Kasparian,¹  and Maura Brunetti^{1,c)} 

AFFILIATIONS

¹Group of Applied Physics and Institute for Environmental Sciences, University of Geneva, 66 Bd Carl-Vogt, CH-1211 Geneva 4, Switzerland

²Department of Mechanical Engineering, Massachusetts Institute of Technology, Cambridge, Massachusetts 02139, USA

³Department of Engineering Science, University of Oxford, Parks Road, Oxford OX1 3PJ, United Kingdom

⁴Laboratory of Theoretical Physics of Nanosystems, EPFL, CH-1015 Lausanne, Switzerland

⁵Disaster Prevention Research Institute & Hakubi Center for Advanced Research, Kyoto University, Kyoto, 606-8501 Kyoto, Japan

⁶School of Civil Engineering, The University of Sydney, Sydney, NSW 2006, Australia

^{a)}Present address: Department of Mathematics and Statistics, University of Reading, Reading, United Kingdom

^{b)}Present address: Department of Engineering, University of Ferrara, via Saragat 1, I-44122 Ferrara, Italy

^{c)}Author to whom correspondence should be addressed: maura.brunetti@unige.ch

ABSTRACT

The evaluation and consideration of the mean flow in wave evolution equations are necessary for the accurate prediction of fluid particle trajectories under wave groups, with relevant implications in several domains, from the transport of pollutants in the ocean to the estimation of energy and momentum exchanges between the waves at small scales and the ocean circulation at large scale. We derive an expression of the mean flow at a finite water depth, which, in contrast to other approximations in the literature, accurately accords with the deep-water limit at third order in steepness and is equivalent to second-order formulations in intermediate water. We also provide envelope evolution equations at fourth order in steepness for the propagation of unidirectional wave groups either in time or space that include the respective mean flow term. The latter, in particular, is required for accurately modeling experiments in water wave flumes in arbitrary depths.

© 2023 Author(s). All article content, except where otherwise noted, is licensed under a Creative Commons Attribution (CC BY) license (<http://creativecommons.org/licenses/by/4.0/>). <https://doi.org/10.1063/5.0164784>

I. INTRODUCTION

As waves evolve on the ocean surface, they induce a mean flow to the fluid particles, particularly when nonlinear effects are taken into account. Near the surface, fluid particles experience a net horizontal displacement in the same direction as the water wave propagation, the so-called Stokes drift,^{1,2} that decays with depth. A return flow in the fluid column along vertical and horizontal directions guarantees the conservation of the water-mass transport, causing localized variations in the mean water level under wave groups and the associated propagation of infragravity waves³ at a finite water depth. An accurate description of the mean flow is, thus, necessary for the proper reconstruction of the fluid particle trajectories underneath water waves.^{4,5} Since the wave-induced mean flow is associated with the transport of energy, momentum, and other tracers,⁶ such as pollutants like plastic⁷

or offshore oil spill,⁸ it is relevant for environmental studies. Moreover, it has an impact on the general circulation of the ocean at large scales and its modeling,^{9–12} and on the nearshore circulation,^{3,13} in particular in shoaling regions,^{14,15} while it is affected by the presence of background shear currents.^{16,17}

Since Stokes drift and return flow are two phenomena occurring at second order in steepness, they are taken into account in the finite water depth nonlinear Schrödinger equation (NLS), which describes the evolution of the envelope of narrow-banded wave packets and can be obtained using a multi-scale development of water surface elevation and velocity potential at third order in steepness,^{18–21} or taking the narrow-banded limit of the Zakharov equation using an Hamiltonian approach.^{22,23} Indeed, at third order in steepness, it was shown²⁰ that the mean flow term comes into play as a modification of the nonlinear

coefficient, giving rise to a transition from focusing to defocusing regimes at the critical value $k_0 h \approx 1.363$, where k_0 is the carrier wavenumber and h the depth. However, this contribution to the nonlinear coefficient disappears in the deep-water limit. At fourth order in steepness, the accurate formulation of the mean flow term needs to be accounted for, in both, finite and infinite depth waters.²⁴

Fourth-order terms in the NLS equation are necessary to explain features like asymmetrical evolution of spectra²⁵ and asymmetries in the waveform,^{26–30} especially when inevitable wave focusing is at play.³¹ Several versions of high-order wave envelope evolution equations exist in the literature, which can be obtained when applying the multiple scales development using steepness and bandwidth with different orders of magnitude^{24,32–34} or the Hamiltonian approach.^{23,35–38} The main difference between all these equations is the treatment and approximation of the mean flow term.

Here, we will focus on narrow-banded unidirectional wave packets where steepness and bandwidth can be considered as parameters of the same order, like in the finite-depth developments described in Refs. 39 (denoted as Sed03 in the following) and 40 (Slu05). The challenge of such developments is the fact that they do not reduce to the Dysthe equation (Ref. 24, Dys79) in the deep-water limit, which has been shown to well reproduce wave tank experiments.²⁸ We will show that this convergence depends on how the mean flow is approximated. Moreover, we will provide finite-depth envelope equations at fourth order in steepness in both space-like and time-like formulations, with correct limiting expressions in deep water. In particular, such unidirectional time-like equations that allow a continuous scaling from intermediate to the deep water limit are relevant for reproducing wave tank experiments with high accuracy in arbitrary depths. In contrast, directional sea states are typically found in the open ocean, and this restricts the applicability of the above unidirectional modeling equations.

The paper is organized as follows: In Sec. II, we will derive the expression of the mean flow to be inserted in the envelope equation at fourth order in steepness for the evolution in time. We will compare this expression with the ones already existing in the literature and show that it indeed correctly describes the mean flow in the whole range of water depths, i.e., from intermediate to deep water regimes. In Sec. III, we will provide an envelope equation for the water wave evolution in space, relevant for modeling, for instance water tank experiments, and the corresponding mean flow term, at fourth order in steepness. Again, we will perform the comparison for various water depth scenarios. Finally, in Sec. IV, we will summarize our findings.

II. FOURTH-ORDER EQUATION: PROPAGATION IN TIME

The multi-scale approach has been used to derive at fourth order in steepness the following equation, which describes the evolution of the envelope U of a unidirectional progressive gravity wave packet propagating in time on the free surface of a homogeneous liquid with depth h ,^{39–41}

$$i \left(\frac{\partial U}{\partial t} + c_g \frac{\partial U}{\partial X} \right) + \hat{\alpha} \frac{\partial^2 U}{\partial X^2} - \underbrace{\hat{\beta} |U|^2 U}_{\text{incl. Mean Flow}} = i \left(\hat{\alpha}_3 \frac{\partial^3 U}{\partial X^3} - \underbrace{\hat{\beta}_{21} |U|^2 \frac{\partial U}{\partial X} - \hat{\beta}_{22} U^2 \frac{\partial U^*}{\partial X}}_{\text{incl. Mean Flow}} \right). \quad (1)$$

The explicit formulation of the group velocity c_g and of all dispersive and nonlinear coefficients $\hat{\alpha}$, $\hat{\beta}$, $\hat{\alpha}_3$, $\hat{\beta}_{21}$, and $\hat{\beta}_{22}$ is given in Appendixes A and B. The surface tension has been neglected, and the fluid is considered as irrotational. The sign convention follows Sed03: The surface elevation is reconstructed at leading order from the envelope using⁴² $\eta(X, t) = \frac{1}{2} [U(X, t) \exp(i(k_0 X - \omega_0 t)) + c. c.]$, where ω_0 and k_0 are the angular frequency and wavenumber of the carrier wave, respectively.

Equation (1) is referred to as the “space-like equation” since dispersion is in space. It can also be written in the following equivalent form³⁹ in a reference frame moving with the group velocity $x = X - c_g t$,

$$i \frac{\partial U}{\partial t} + \varepsilon \left(\hat{\alpha} \frac{\partial^2 U}{\partial x^2} - \hat{\beta}_D |U|^2 U \right) = i \varepsilon^2 \left(\hat{\alpha}_3 \frac{\partial^3 U}{\partial x^3} - \omega_0 k_0 \tilde{Q}_{41} |U|^2 \frac{\partial U}{\partial x} - \omega_0 k_0 \tilde{Q}_{42} U^2 \frac{\partial U^*}{\partial x} \right) + \underbrace{\frac{\mu_g k_0}{4\sigma} U \frac{\partial \phi_0}{\partial x}}_{\text{Mean Flow}}, \quad (2)$$

where $\sigma = \tanh(k_0 h)$, μ_g is given in Eq. (A15), and the high-order nonlinear coefficients \tilde{Q}_{41} and \tilde{Q}_{42} in Eqs. (B4) and (B7), respectively. The nonlinear term $\hat{\beta}_D$ is a positive function (see Fig. 1), given in Eq. (A9), and since the dispersion coefficient $\hat{\alpha}$ is negative, it seems that the characterization of the focusing and defocusing regime is somehow lost in the present formulation.

Notice that we explicitly introduce the scaling parameter ε , a dummy variable which is set to 1 at the end, that is helpful for grouping terms of the same order in steepness. The last term, depending on the zero harmonic of the velocity potential ϕ_0 , is the mean flow term that, from the multi-scale development, takes the following form [see Eqs. (35) and (57) in Sed03]:

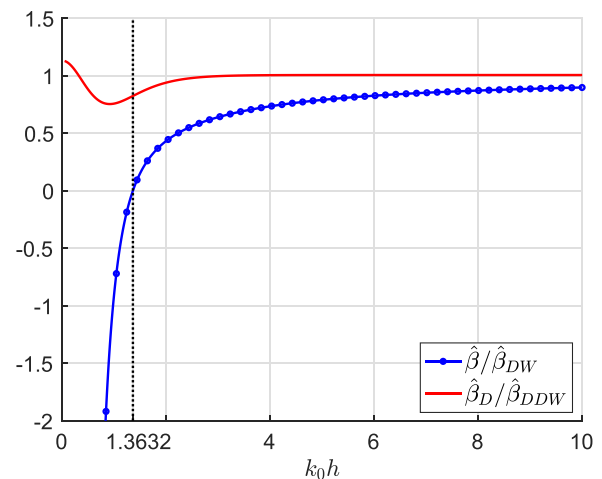


FIG. 1. Third-order nonlinear coefficients $\hat{\beta}$ and $\hat{\beta}_D$ in Eqs. (1) and (2), respectively, normalized with respect to their deep-water values, which are equal. Zero crossing for $\hat{\beta}$ is at $k_0 h = 1.363$, shown by the dotted vertical line.

$$\frac{\partial \phi_0}{\partial x} = \varepsilon \frac{\omega_0 \mu_s k_0}{2 \sigma \nu} |U|^2 - i \varepsilon^2 \frac{4 \omega_0 \sigma}{\nu} \tilde{q}_{40S} \left(U \frac{\partial U^*}{\partial x} - U^* \frac{\partial U}{\partial x} \right), \quad (3)$$

with ν given in Eq. (A16) and \tilde{q}_{40S} in Eq. (B10). Its contribution can be included into the coefficients $\tilde{\beta}_D, \tilde{Q}_{41}, \tilde{Q}_{42}$ to obtain $\hat{\beta}, \hat{\beta}_{21}, \hat{\beta}_{22}$, respectively, in Eq. (1) [see steps from Eqs. (40) to (42) and from Eqs. (64) to (66) in Sed03]. Thus, the mean flow term is already taken into account in Eq. (1) at fourth order in steepness through the nonlinear coefficients.

We remark that from Eq. (3), in the deep-water limit, $\partial \phi_0 / \partial x \rightarrow 0$ since $\nu \rightarrow -\infty$, while all the other coefficients are finite. This agrees with the developments at third order in steepness.^{20,43} Note that in the 1D shallow-water case, the mean flow term modifies the nonlinear term, see Eq. (2.21) in Ref. 20, while its contribution vanishes in the deep-water limit. However, the fact that the contribution of mean flow remains zero in deep water at higher-order approximation in steepness is not ideal, as we will discuss in the following subsection.

A. Mean flow in the deep-water limit

In the Dysthe equation (Dys79), i.e., the evolution equation obtained in the deep-water limit with the multi-scale method at fourth order in steepness, an additional term corresponding to the wave-induced mean flow usually appears in the literature in both space-like^{24,32,44} and time-like 1D formulations.^{28,45–48} Let us consider for the moment the propagation in time. The Dysthe equation reads

$$\begin{aligned} i \frac{\partial U}{\partial t} - \frac{\omega_0}{8k_0^2} \frac{\partial^2 U}{\partial x^2} - \frac{\omega_0 k_0^2}{2} |U|^2 U \\ = i \frac{\omega_0}{16k_0^3} \frac{\partial^3 U}{\partial x^3} - i \frac{\omega_0 k_0}{2} \left(3|U|^2 \frac{\partial U}{\partial x} + \frac{1}{2} U^2 \frac{\partial U^*}{\partial x} + \underbrace{\frac{2i}{\omega_0} U \frac{\partial \phi_0}{\partial x}}_{\text{Mean Flow}} \right). \end{aligned} \quad (4)$$

In this deep-water limit, the mean-flow term is written as^{28,47}

$$\left. \frac{\partial \phi_0}{\partial x} \right|_{z=0} = \frac{\omega_0}{2} \mathcal{H}_x \left[\frac{\partial |U|^2}{\partial x} \right], \quad (5)$$

where \mathcal{F}_x is the Fourier transform in space, and \mathcal{H}_x the Hilbert transform, $\mathcal{H}_x[\eta] = \mathcal{F}_x^{-1} [+i \operatorname{sgn}(k) \mathcal{F}_x[\eta]]$, with η being a function of x . The role of the mean flow Hilbert term in the evolution of pulsating wave packets²⁵ and narrow-banded irregular waves^{27,28} has been shown in several experiments in deep water, and its presence is required for a correct modeling.²⁶

Janssen³² suggested that the system can be closed by solving the equations for ϕ_0 as a function of the envelope U in the Fourier space. It is instructive to report here the explicit derivation of the Hilbert term since we will use analogous developments in the following. The zero harmonic of the velocity potential ϕ_0 satisfies the Laplace equation in the entire water column with boundary conditions at the surface and at the bottom, giving a set of equations that constitutes the following Neumann problem:

$$\frac{\partial^2 \phi_0}{\partial z^2} + \frac{\partial^2 \phi_0}{\partial x^2} = 0 \quad -\infty < z \leq 0, \quad (6a)$$

$$\frac{\partial \phi_0}{\partial z} = \frac{\omega_0}{2} \frac{\partial |U|^2}{\partial x} \quad z = 0, \quad (6b)$$

$$\frac{\partial \phi_0}{\partial z} = 0 \quad z \rightarrow -\infty \quad (6c)$$

Substituting the Fourier transform of the mean flow

$$\mathcal{F}_x \phi_0(x, z, t) = \hat{\phi}_0(k, z, t) = \frac{1}{\sqrt{2\pi}} \int_{-\infty}^{\infty} \phi_0(x, z, t) e^{ikx} dx \quad (7)$$

into the Laplace equation gives $\partial^2 \hat{\phi}_0 / \partial z^2 = k^2 \hat{\phi}_0$ whose solution is

$$\hat{\phi}_0(k, z, t) = C_1 e^{|k|z} \quad (8)$$

with C_1 independent of z . This satisfies the bottom boundary condition for $z \rightarrow -\infty$.

Inserting this expression in Eq. (6b) gives

$$|k| C_1 e^{|k|z} \Big|_{z=0} = |k| C_1 = \frac{\omega_0}{2} \mathcal{F}_x \left[\frac{\partial |U|^2}{\partial x} \right], \quad (9)$$

from which C_1 is obtained, and thus,

$$\hat{\phi}_0(k, z, t) = \frac{1}{|k|} \frac{\omega_0}{2} e^{|k|z} \mathcal{F}_x \left[\frac{\partial |U|^2}{\partial x} \right]. \quad (10)$$

Now the derivative with respect to x at $z=0$ in the Fourier space is given by

$$\mathcal{F}_x \left[\frac{\partial \phi_0}{\partial x} \right] \Big|_{z=0} = ik \hat{\phi}_0 \Big|_{z=0} = i \frac{\omega_0}{2} \operatorname{sgn}(k) \mathcal{F}_x \left[\frac{\partial |U|^2}{\partial x} \right], \quad (11)$$

and finally, moving back to the direct physical space, the Hilbert term of Eq. (5) is recovered.

B. Multi-scale development and Hilbert term

As discussed, the multi-scale approach of Sed03 gives Eq. (3), which in the deep-water limit reduces to

$$\frac{\partial}{\partial x} (\phi_{01} + \phi_{02}) = 0. \quad (12)$$

On the other hand, the mean flow can be written as the Hilbert term of Eq. (5) in the Dysthe equation.^{24,32} Thus, there is the need to reconcile these results. This can be done as follows. In the derivation of the Hilbert term, we use the Laplace equation for ϕ_0 that is the complete mean flow, and not just its approximation at second order in steepness as in Eq. (12). Indeed, the Laplace equation at third order for the mean flow is

$$\frac{\partial^2 \phi_{03}}{\partial z^2} + \frac{\partial^2 \phi_{01}}{\partial x^2} = 0. \quad (13)$$

When integrated in z , this gives

$$\frac{\partial \phi_{03}}{\partial z} = -(z+h) \frac{\partial^2 \phi_{01}}{\partial x^2}, \quad (14)$$

using the fact that $\partial \phi_{01} / \partial z = 0$ and imposing the bottom boundary condition. From the multi-scale development, the following expression can be obtained at third order in steepness [see Eqs. (2.12) and (2.14) in Ref. 20]:

$$\frac{c_g^2}{g} \frac{\partial^2 \phi_{01}}{\partial x^2} + \frac{\partial \phi_{03}}{\partial z} = \frac{\omega_0}{2\sigma} (1 + C_{FD}) \frac{\partial |U|^2}{\partial x} = D' \frac{\partial |U|^2}{\partial x}, \quad (15)$$

with the coefficient C_{FD} defined in Eq. (A17) and in Ref. 4, where $D' = (1 + C_{FD}) \omega_0 / (2\sigma) = \mu_g \omega_0 / (8\sigma^2)$ (see definitions in Appendix A). Using Eq. (14) at $z = 0$, Eq. (15) reduces to

$$\frac{\partial^2 \phi_{01}}{\partial x^2} = -\frac{D}{h} \frac{\partial |U|^2}{\partial x}, \tag{16}$$

which corresponds to Eqs. (33) and (34) in Sed03, where D is defined in Eq. (A13). Equation (16) can also be written, using Eq. (14), as

$$\frac{\partial \phi_{03}}{\partial z} = D \frac{\partial |U|^2}{\partial x}. \tag{17}$$

Taking the deep-water limit gives Eq. (6b), i.e., the boundary condition at the surface in the Neumann problem. Since $\partial \phi_{01} / \partial z = 0$ and $\partial \phi_{02} / \partial z = 0$, such expression is valid at third order in steepness for the mean flow.

Thus, in the derivation of the Hilbert term, the complete mean flow (in the Laplace equation) is considered together with the mean flow at third order in steepness in the surface boundary condition. Consequently, a ‘‘hybrid’’ relation as described by Eq. (5) is obtained, which is different from Eq. (12) where only the first terms in the development of the mean flow at the surface are taken into account. In other words, the expression in Eq. (5) is inherently nonlocal. The same occurs in the nonlinear terms of the supercompact model,⁴⁹ from which the Dysthe equation can be derived. The terms in Sed03 and Slu05 are instead local, as they only involve the surface, and not the entire water column. This is obviously an approximation, since the mean flow does involve a body of fluid, which is not immediately at the surface, as clearly shown in field measurements.³

C. Mean flow term in arbitrary depth

We now repeat the procedure used in Sec. II A for the case of intermediate water. We will consider two cases that differ based on the considered surface boundary condition: The Neumann problem is solved using the condition given by Eq. (17) in case 1, using Eq. (15) in case 2. Replacing the expression of $\partial \phi_0 / \partial x$ that is obtained in each case into the last term of Eq. (2) gives the final high-order NLS equation in an arbitrary finite depth and in the space-like form.

1. Case 1

Moving as before to the Fourier space, the Laplace equation is $\partial^2 \hat{\phi}_0 / \partial z^2 = k^2 \hat{\phi}_0$ and its solution is given by

$$\hat{\phi}_0(k, z, t) = C_1 e^{k(z+h)} + C_2 e^{-k(z+h)}. \tag{18}$$

Imposing the boundary condition at the bottom, Eq. (6c), gives

$$\frac{\partial \hat{\phi}_0}{\partial z} \Big|_{z=-h} = |k|(C_1 - C_2) = 0. \tag{19}$$

Thus, we have $C_1 = C_2 = C/2$ and

$$\hat{\phi}_0(k, z, t) = C \cosh(|k|(z+h)). \tag{20}$$

Inserting this in Eq. (17) gives

$$|k|C \sinh(|k|(z+h)) \Big|_{z=0} = D \mathcal{F}_x \left[\frac{\partial |U|^2}{\partial x} \right], \tag{21}$$

from which one obtains C and therefore,

$$\hat{\phi}_0 = \frac{1}{|k|} \frac{\cosh(|k|(z+h))}{\sinh(|k|h)} D \mathcal{F}_x \left[\frac{\partial |U|^2}{\partial x} \right]. \tag{22}$$

At $z = 0$, this gives

$$\hat{\phi}_0 \Big|_{z=0} = D \frac{\coth(|k|h)}{|k|} \mathcal{F}_x \left[\frac{\partial |U|^2}{\partial x} \right]. \tag{23}$$

Now, the derivative with respect to x at $z = 0$ is given by

$$\mathcal{F}_x \left[\frac{\partial \hat{\phi}_0}{\partial x} \right] \Big|_{z=0} = ik \hat{\phi}_0 \Big|_{z=0} = iD \frac{\text{sgn}(k)}{\tanh(|k|h)} \mathcal{F}_x \left[\frac{\partial |U|^2}{\partial x} \right]. \tag{24}$$

Moving back to the direct physical space, we finally get

$$\frac{\partial \phi_0}{\partial x} = D \mathcal{F}_x^{-1} \left\{ \frac{i}{\tanh(kh)} \mathcal{F}_x \left[\frac{\partial |U|^2}{\partial x} \right] \right\}. \tag{25}$$

2. Case 2

The surface boundary condition is now Eq. (15). Note that the relation $\phi_{03z} = -h\phi_{01xx}$ has not been used to simplify the lhs of this equation, and both mean flow terms are, thus, considered being of the same order, see Eq. (13) in Ref. 4.

Inserting the generic form of the solution in intermediate water, i.e., Eq. (20), into the surface boundary condition, Eq. (15), gives

$$C \left[\frac{c_g^2}{g} (-k^2) \cosh(|k|(z+h)) + |k| \sinh(|k|(z+h)) \right] \Big|_{z=0} = D' \mathcal{F}_x \left[\frac{\partial |U|^2}{\partial x} \right], \tag{26}$$

from which we obtain the following expression for $C(k, t)$:

$$C(k, t) = \frac{D'}{k \tanh(kh) [1 - c_g^2 k / (g \tanh(kh))]} \frac{1}{\cosh(kh)} \mathcal{F}_x \left[\frac{\partial |U|^2}{\partial x} \right], \tag{27}$$

where we used $|k| \tanh(|k|h) = k \tanh(kh)$, and c_g is the wave group speed at the carrier wavenumber. Performing analogous steps as in the previous case, the final expression for the Euler horizontal velocity in $z = 0$ is

$$\frac{\partial \phi_0}{\partial x} = D' \mathcal{F}_x^{-1} \left\{ \frac{i}{\tanh(kh) [1 - c_g^2 k / (g \tanh(kh))]} \mathcal{F}_x \left[\frac{\partial |U|^2}{\partial x} \right] \right\}. \tag{28}$$

Note that this expression coincides with Eq. (15) in Ref. 4 (apart from a sign that is a typo in that latter equation).

By performing the derivative in x on the rhs of Eqs. (25) or (28), considering that $D = D' / (1 - c_g^2 / (gh))$ and using $\coth y = 1/y + O(y)$, we get in both cases 1 and 2 for small kh numbers,

$$\begin{aligned} \frac{\partial \phi_0}{\partial x} &\sim D\mathcal{F}_x^{-1}[i(ik)\coth(kh)\mathcal{F}_x[|U|^2]] \\ &\sim D\mathcal{F}_x^{-1}\left[-\frac{1}{h}\mathcal{F}_x[|U|^2]\right] \\ &= -\frac{D}{h}|U|^2 = \frac{\omega_0 \mu_g k_0}{2 \sigma \nu}|U|^2. \end{aligned} \tag{29}$$

Thus, we recover the first term on the rhs of Eq. (3). The NLS nonlinear coefficient is also recovered when the mean flow term is added to the third-order nonlinear term in Eq. (2), since $\hat{\beta} = \hat{\beta}_D + D^2\nu/(2h^2\omega_0)$. Hence, the defocusing regime is recovered through the inclusion of the mean flow term.

D. Numerical comparisons

We compare the expressions for the horizontal velocity $\partial\phi_0/\partial x$ listed in Table I with the sub-harmonic velocity potential ϕ_{20} at second order in steepness and its horizontal derivative calculated using the Dalzell analytical method [see the original paper, Ref. 50 (Dal99), and the explicit formulas reported in the Appendix of Ref. 51].

For benchmarking and validation purposes, we use the same parameters as in Ref. 51 (case C in their Table II), namely, a Gaussian (amplitude) spectrum $S(k)$ with peak wavenumber $k_0 = 0.0277 \text{ m}^{-1}$, wavelength $\lambda_0 = 2\pi/k_0$, standard deviation of the spectrum given by symmetrical values $k_w = k_{w1} = k_{w2} = 0.27k_0$, steepness $\varepsilon = 0.3$, and different values of the normalized depth k_0h in the range [0.5, 50], thus the case of finite and infinite water depth conditions. The angular frequency is calculated from $\omega_0^2 = gk_0 \tanh(k_0h)$. In particular, the surface elevation at first order in steepness given by the superposition of $N = 30$ waves is used to calculate the intensity of wave envelope, i.e., $|U|^2$, and then, the horizontal velocity $\partial\phi_0/\partial x$ through the different relations, as listed in Table I. We consider a focused wave group, composed of N individual sinusoidal wave components that are in phase at a single point in time and space⁵² (the origin in our case), and a random sea state by using a uniform distribution for the phases. An example of sea state realization is given in Appendix D.

The results are summarized in Fig. 2 for waves focusing at $x = 0$, and in Fig. 3 for the case of waves superposition with random phases. In both cases, we see that the horizontal velocity calculated by Eq. (29) (gray line), which corresponds to the second-order expression in Sed03, reproduces well the Dalzell waveform (green line) only for $k_0h \leq 2$ and cannot be applied in deep water where it gives a waveform amplitude much smaller than Dysthe’s result (black line). On the contrary, Dysthe’s expression should not be used for $k_0h < 10$ as in our considered cases, especially for large amplitude waveforms, where it does not attain Dalzell’s accuracy. Although an elementary consideration of the dispersion relation suggests that $k_0h \approx 5$ should be

TABLE I. List of mean flow terms in space-like formulation: $\partial\phi_0/\partial x$.

Case 1	Eq. (25)	Third-order, nonlocal
Case 2	Eq. (28)	Third-order, nonlocal
Dys79 (Ref. 24)	Eq. (5)	Third-order, nonlocal deep water
Sed03 (Ref. 39)	Eq. (3)	Third-order
Sed03	Eq. (29)	Second-order
Slu05 (Ref. 40)	Eq. (C10)	Third-order

TABLE II. List of mean flow terms in time-like formulation: $\partial\phi_0/\partial t$.

Case 1	Eq. (39)	Third-order, non-instantaneous
Case 2	Eq. (40)	Third-order, non-inst.
Dys79 (Ref. 24)	Eq. (36)	Third-order, non-inst. deep water
Sed03 (Ref. 39)	Eq. (38)	Third-order
Sed03	1st term on rhs of Eq. (38)	Second-order
Slu05 (Ref. 40)	Eq. (C11)	Third-order

indistinguishable from $k_0h \rightarrow \infty$, the dynamics of the mean flow is consistently different from this limit up to $k_0h = 10$. The expressions for the horizontal velocity given by case 1 [Eq. (25)] and case 2 [Eq. (28)] behave in a similar way at all depths, providing in general an approximation that corresponds well to the Dalzell solution in intermediate waters, and to Dysthe in deep waters. It is also important to note that the expressions provided in Sed03 and Slu05 at third order in steepness [Eqs. (3) and (C10), respectively], give different results and do not correspond to the other models at any depth.

More detailed features can be deduced from Fig. 4, where the deviation operator with respect to the Dysthe expression, defined as $D_{Dysthe} = N^{-1} \int (\phi_{0x} - \phi_{0x}^{Dysthe})^2 dx$, and to the Dalzell one, $D_{Dalzell} = N^{-1} \int (\phi_{0x} - \phi_{0x}^{Dalzell})^2 dx$, with $\phi_{0x} = \partial\phi_0/\partial x$, is shown as a function of the non-dimensional water depth k_0h . The integral is calculated over $L = 80\lambda_0$, and the normalization coefficient is $N = (\omega_{0DW}\lambda_0)^2 L$, with ω_{0DW} calculated in deep water (DW). The Stokes series expansion of the velocity potential (and thus Dalzell’s model) converges in shallow water⁵³ if $3\varepsilon/(2k_0h)^3 \ll 1$, thus at low Ursell number, which implies in our case $k_0h \gg 0.48$. This region is excluded in Fig. 4. It can be seen that the expression for the horizontal velocity given by case 2 [Eq. (28)] is accurate at second order at all depths, almost superposing to the second-order Dalzell solution, while the one given by case 1 [Eq. (25)] is the only expression that consistently converges to the Dysthe in the deep-water limit expression and is equivalent to case 2 for $k_0h < 5$. Note that the third-order corrections provided in Sed03 [Eq. (3)] and in Slu05 [Eq. (C10)] are different and do not extend the validity to deeper water regimes of the second-order expression [Eq. (29)], which is accurate for $k_0h < 2$ [see Fig. 4(b)]. This raises a warning on the quantitative accuracy of these third-order expressions.

III. FOURTH-ORDER EQUATION: PROPAGATION IN SPACE

In order to transform Eq. (1) to an expression describing the propagation in space, that is necessary to describe the nonlinear evolution of waves in a laboratory flume, a change of variables is needed,

$$\tau = \varepsilon \left(t - \frac{x}{c_g} \right); \quad \xi = \varepsilon^2 x. \tag{30}$$

Through this transformation, the third-order terms are only subject to a rescaling,

$$\alpha = \frac{\hat{\alpha}}{c_g^3}; \quad \beta = \frac{\hat{\beta}}{c_g}. \tag{31}$$

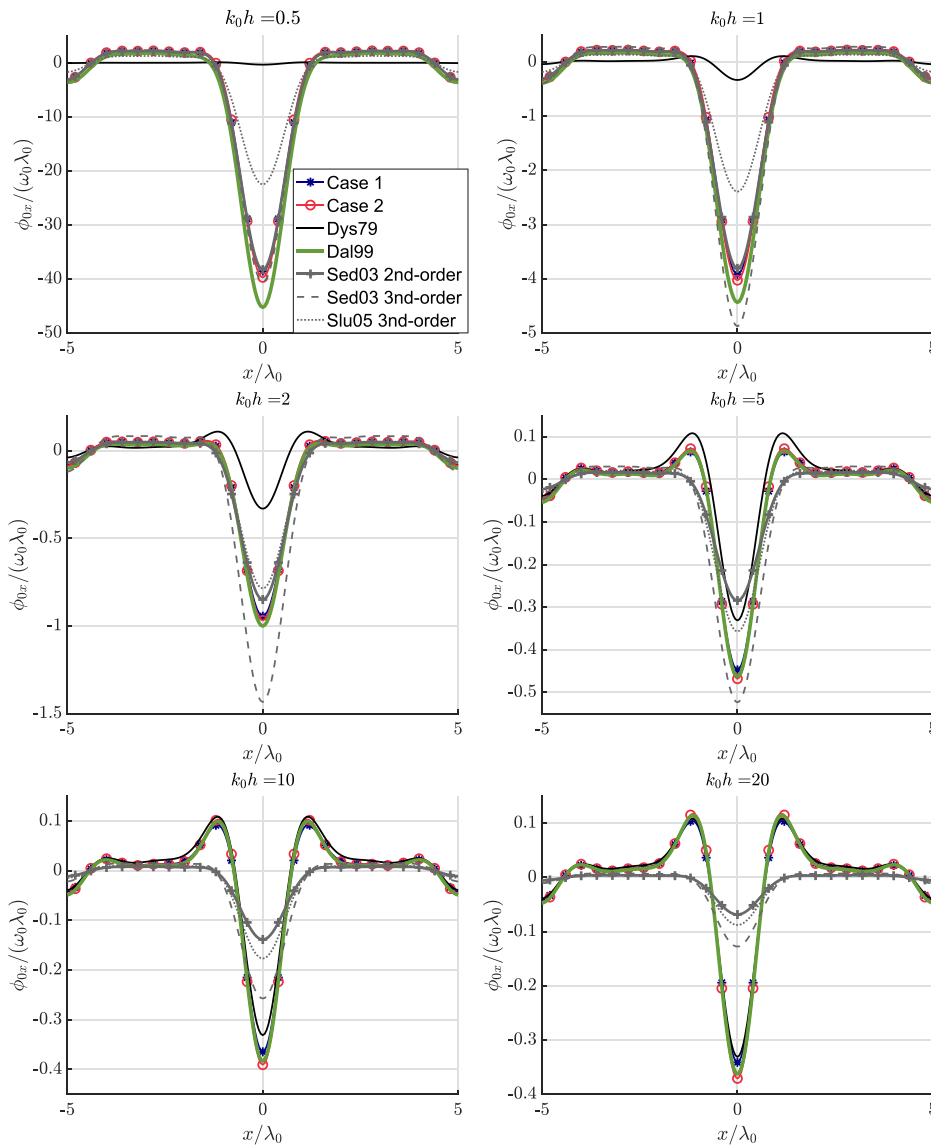


FIG. 2. Mean flow ϕ_{0xz} for $N=30$ waves focusing at $x=0$ as described by the expressions listed in Table 1, for different values of k_0h .

The higher-order terms are instead dramatically modified. Indeed, a mixed derivative appears from the second-order dispersion term, $\partial^2 U/\partial x^2$, that reads as $-(\omega''/c_g)\partial^2 U/\partial x\partial t$. In the multiscale spirit, the time-like NLS (i.e., terms at third order in steepness) is used to estimate this term, which results in corrections at fourth order. The resulting time-like form of the evolution equation does not appear explicitly in the literature and is given by (setting $\varepsilon = 1$, and changing the notation as $\tau \rightarrow t$ and $\xi \rightarrow x$)

$$i\frac{\partial U}{\partial x} + \alpha\frac{\partial^2 U}{\partial t^2} \underbrace{-\beta|U|^2 U}_{\text{incl. Mean Flow}} = -i\alpha_3\frac{\partial^3 U}{\partial t^3} + \underbrace{i\beta_{21}|U|^2\frac{\partial U}{\partial t} + i\beta_{22}U^2\frac{\partial U^*}{\partial t}}_{\text{incl. Mean Flow}}, \quad (32)$$

whose dispersion and nonlinear coefficients are given in Appendixes A and B, and their dependence on k_0h is shown in Figs. 5 and 6.

High-order dispersion terms⁵⁴ are easily included up to arbitrary order following Refs. 55 and 56, reducing the constraints in the bandwidth of the original Dysthe equation.

Using the relation³⁹

$$\frac{\partial \phi_{01}}{\partial t} = -c_g \frac{\partial \phi_{01}}{\partial x}, \quad (33)$$

Eq. (32) can be rewritten in the following equivalent form:

$$i\frac{\partial U}{\partial x} + \alpha\frac{\partial^2 U}{\partial t^2} - \beta_D|U|^2 U = -i\alpha_3\frac{\partial^3 U}{\partial t^3} + iB_{21}|U|^2\frac{\partial U}{\partial t} + iB_{22}U^2\frac{\partial U^*}{\partial t} - \underbrace{\frac{\mu_g k_0}{4\sigma c_g^2} U \frac{\partial \phi_0}{\partial t}}_{\text{Mean Flow}}, \quad (34)$$

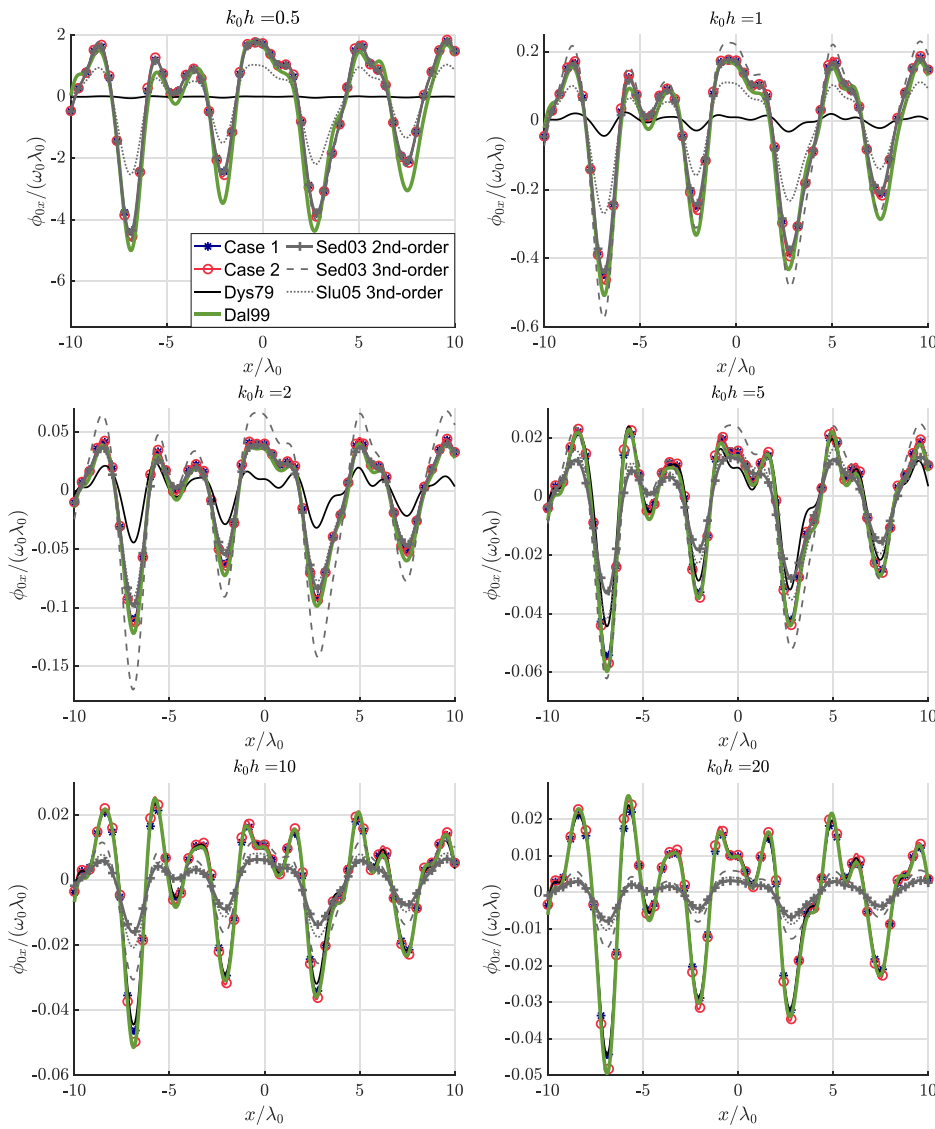


FIG. 3. The same as Fig. 2 for the evolution of $N=30$ waves with random phases.

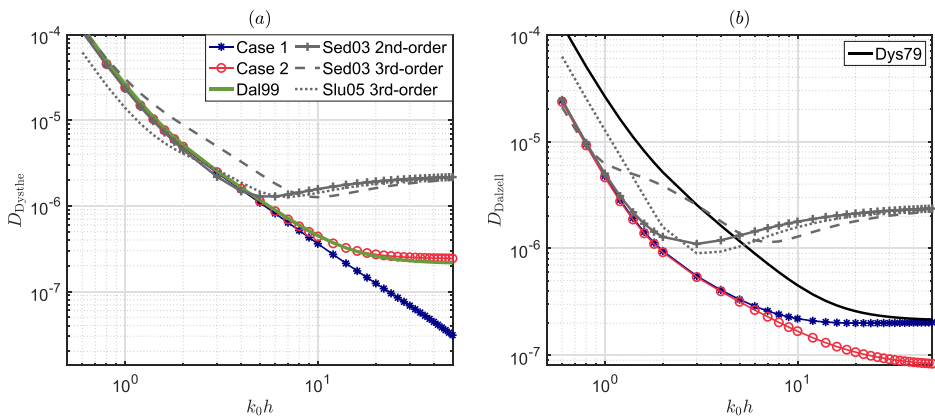


FIG. 4. Deviation operator with respect to the Dysthe expression (a) and to the Dalzell one (b) for the derivative in space ϕ_{0x} , as defined in the main text, for the different cases listed in Table I.

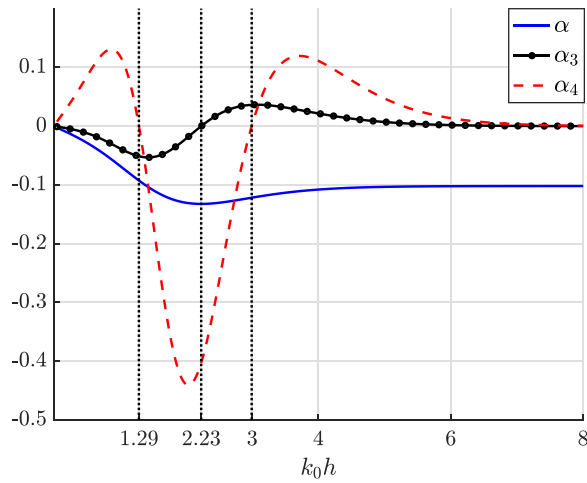


FIG. 5. Dispersion coefficients (for $\omega_0 = 1$ Hz). Zero crossings are marked on the horizontal axis.

where $\beta_D = \hat{\beta}_D/c_g$, $\mathcal{B}_{21} = \omega_0 k_0 \tilde{Q}_{41}/c_g^2 - 4\alpha\beta_D c_g$, $\mathcal{B}_{22} = \omega_0 k_0 \tilde{Q}_{42}/c_g^2 - 2\alpha\beta_D c_g$, with $\hat{\beta}_D$, α , α_3 given in Appendix A and \tilde{Q}_{41} , \tilde{Q}_{42} in Appendix B. The dependence of the nonlinear coefficients on $k_0 h$ is illustrated in Fig. 6. Note that β , β_{21} , β_{22} , \mathcal{B}_{21} , and \mathcal{B}_{22} diverge quite strongly for $k_0 h \rightarrow 0$, i.e., particularly in the defocusing regime. That said and as can be also analytically verified, all coefficients correctly reproduce their deep-water limit at $k_0 h \rightarrow \infty$.

A. Mean flow in time-like equations

At main order in steepness, Eqs. (3) and (33) imply

$$\frac{\partial |U|^2}{\partial t} = -c_g \frac{\partial |U|^2}{\partial x}. \tag{35}$$

Thus, ϕ_{01} and $|U|^2$ do not depend on x and t separately, but only through their combination $(x - c_g t)$, so that at the leading order, the Fourier transform in space, \mathcal{F}_x , can be replaced by the Fourier transform in time, \mathcal{F}_t . From Eq. (5), in the deep-water limit, it is possible to simply exchange the derivative with respect to space with that with respect to time and vice versa, since the Hilbert transform of the

derivative is the derivative of the Hilbert transform, i.e., these two linear operators commute. As such,

$$\frac{\partial \phi_0}{\partial t} = \frac{\omega_0}{2} \mathcal{H}_t \left[\frac{\partial |U|^2}{\partial t} \right]. \tag{36}$$

The time-like Dysthe equation is given by the deep-water limit of Eq. (34) and reads, using the above-mentioned expression for the mean flow term,^{28,45–48}

$$i \frac{\partial U}{\partial x} - \frac{k_0}{\omega_0^2} \frac{\partial^2 U}{\partial t^2} - k_0^3 |U|^2 U = 2i \frac{k_0^3}{\omega_0} \left(4|U|^2 \frac{\partial U}{\partial t} + U^2 \frac{\partial U^*}{\partial t} + \underbrace{iU \mathcal{H}_t \left[\frac{\partial |U|^2}{\partial t} \right]}_{\text{Mean Flow}} \right), \tag{37}$$

where $\alpha_3 \rightarrow 0$, since $k \propto \omega^2$, and $\hat{\beta}_{21} \rightarrow \frac{3}{2} \omega_0 k_0$, $\hat{\beta}_{22} \rightarrow \frac{1}{4} \omega_0 k_0$, $\beta_{21} \rightarrow 8k_0^3/\omega_0$, and $\beta_{22} \rightarrow 2k_0^3/\omega_0$.

For the last term in Eq. (34), the Sed03 expression, as in Eq. (3), can be written in terms of the time derivative, using Eq. (33),

$$\frac{\partial \phi_0}{\partial t} = -c_g \frac{\omega_0 k_0 \mu_g}{2 \sigma \nu} |U|^2 - i \frac{4\omega_0 \sigma}{\nu} \tilde{q}_{40S} \left(U \frac{\partial U^*}{\partial t} - U^* \frac{\partial U}{\partial t} \right). \tag{38}$$

However, this expression goes to zero in the deep-water limit, and thus, it does not converge to the Dysthe mean flow given in Eq. (36).

Replacing Eq. (33) in the Laplace equation and the surface boundary conditions, and repeating the same steps of Sec. II C, we finally get the following expressions for the derivative in time of ϕ_0 for cases 1 and 2, respectively, to be inserted in the evolution equation [Eq. (34)]:

$$\frac{\partial \phi_0}{\partial t} = D \mathcal{F}_t^{-1} \left\{ \frac{i}{\tanh(\omega h/c_g)} \mathcal{F}_t \left[\frac{\partial |U|^2}{\partial t} \right] \right\}, \text{ for case 1,} \tag{39}$$

$$\frac{\partial \phi_0}{\partial t} = D' \mathcal{F}_t^{-1} \left\{ \frac{i}{\tanh(\omega h/c_g) [1 - c_g \omega / (g \tanh(\omega h/c_g))]} \mathcal{F}_t \left[\frac{\partial |U|^2}{\partial t} \right] \right\}, \text{ for case 2.} \tag{40}$$

B. Numerical comparisons

We now compare the expressions for $\partial \phi_0 / \partial t$ listed in Table II with the sub-harmonic velocity potential ϕ_{20} at second order in

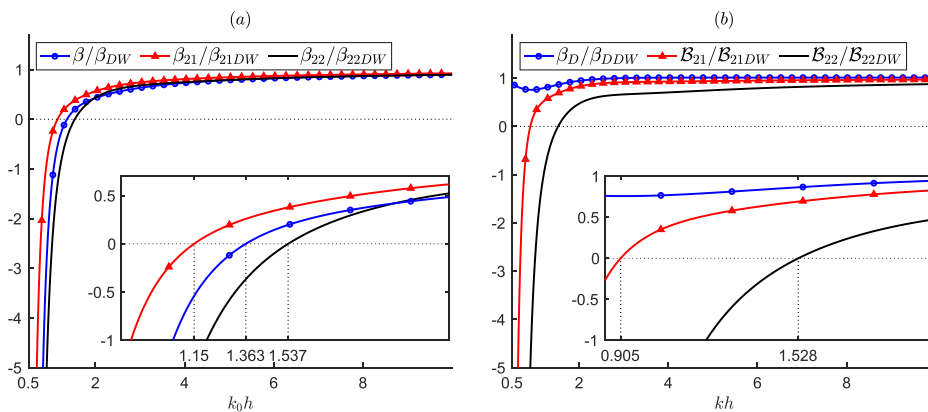


FIG. 6. Nonlinear coefficients (a) in Eq. (32), and (b) in Eq. (34), normalized with respect to their deep-water values [in Dysthe equation, Eq. (37)]. Zero crossings are marked in the insets.

03 November 2023 13:25:55

steepness and its time derivative calculated using the Dalzell analytical method in Refs. 50 and 51.

We use the same parameters as in Sec. II D, starting in this case by a Gaussian (amplitude) spectrum $S(\omega)$ peaked at $\omega_0 = 1$ Hz.

The results for $N=30$ waves focusing at $t=0$ are shown in Fig. 7. We see that the second-order expression in Sed03 reproduces well the waveform only for $k_0h \leq 1$, showing discrepancies with respect to Dalzell's solution at $k_0h = 2$ and not converging to Dysthe's solution in deep water. As for the space-like form, the expressions for ϕ_{0t} given by case 1 [Eq. (39)] and case 2 [Eq. (40)] have a similar behavior at all depths, providing in general approximations that are as accurate as the Dalzell solution in intermediate waters, and as the Dysthe expression at deep waters. As before, the third-order expressions provided by Eqs. (38) and (C11) are different and do not correspond to the other models. Figure 8 shows the deviation operator with respect to the Dysthe expression, defined similarly to the spatial

counterpart (see Sec. II D) as $D_{Dysthe} = N^{-1} \int (\phi_{0t} - \phi_{0t}^{Dysthe})^2 dt$, and to the Dalzell one, $D_{Dalzell} = N^{-1} \int (\phi_{0t} - \phi_{0t}^{Dalzell})^2 dt$ as a function of the non-dimensional water depth k_0h . The integral is now calculated over $T = 80 T_0$, and the normalization coefficient is $N = (\omega_0 \lambda_{0DW})^4 T$, with λ_{0DW} calculated at deep water. As for the space-like case, it can be seen that the expression given by case 2 [Eq. (40)] is accurate at second order at all depths as the second-order Dalzell solution, while the one given by case 1 [Eq. (39)] is the only expression that converges to the Dysthe term in the deep-water limit and is equivalent to case 2 for $k_0h < 3$.

IV. CONCLUSION

During the evolution of surface gravity waves, fluid particles experience Stokes drift along the propagation direction of the waves and a return flow in vertical and horizontal directions, which closes

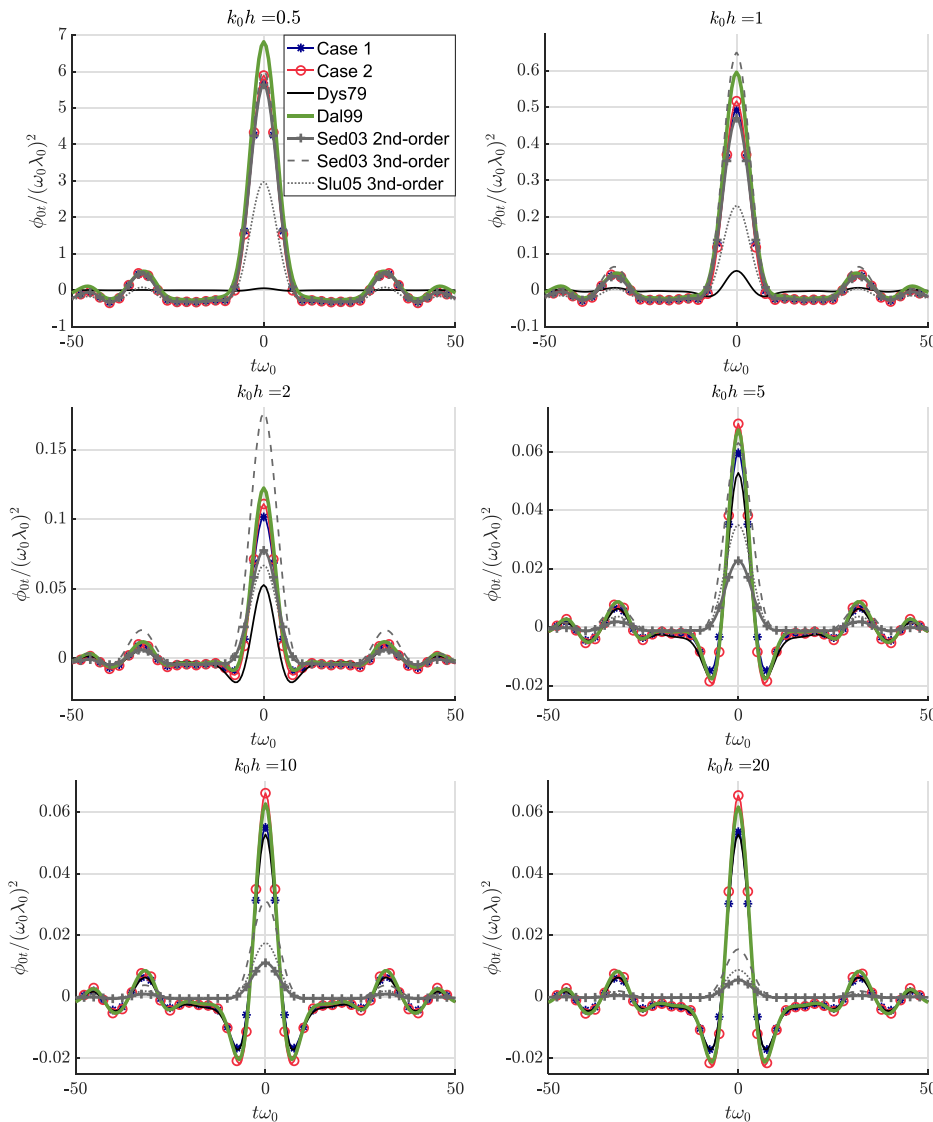


FIG. 7. Mean flow ϕ_{0t} for $N=30$ waves focusing at $t=0$ described by the expressions listed in Table II, for different values of k_0h .

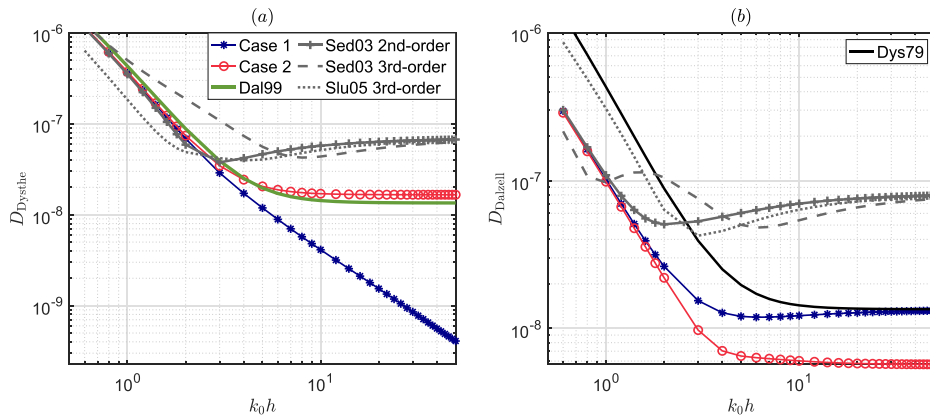


FIG. 8. Deviation operator with respect to the Dysthe expression (a) and to the Dalzell one (b) for the derivative in time ϕ_{0t} , as defined in the main text, for the different cases listed in Table II.

the water-mass transport. Both processes give rise to a mean flow at the surface that needs to be accounted for in order to accurately predict the transport of pollutants^{5–8} (such as oil and microplastics) and, more in general, the impact of waves evolution at small scale on the ocean circulation at large scale.^{9–12} We have derived nonlocal (viz. non-instantaneous) expressions of the mean flow [Eqs. (25) and (39)] that correctly converge to the deep-water limit at third order in steepness, while being equivalent to second-order formulations in intermediate waters. We have included these expressions in an envelope evolution equation at fourth order in steepness in both, space-like [Eq. (2)] and time-like [Eq. (34)] formulations. We emphasize that the time-like form is relevant to study the evolution of unidirectional wave groups in space, thus for modeling experiments in water wave flumes at high accuracy in arbitrary depths. Future work will be focusing on the experimental validation of our results in different water depth regimes.

ACKNOWLEDGMENTS

A.G., J.K., and M.B. acknowledge financial support from the Swiss National Science Foundation (Project No. 200020-175697). D.E. acknowledges financial support from the Swiss National Science Foundation (Fellowship No. P2GEP2-191480). A.C. acknowledges support from Kyoto University’s Hakubi Center for Advanced Research.

AUTHOR DECLARATIONS

Conflict of Interest

The authors have no conflicts to disclose.

Author Contributions

Alexis Gomel: Conceptualization (equal); Formal analysis (equal); Investigation (equal); Writing – original draft (supporting); Writing – review & editing (equal). **Corentin Montessuit:** Formal analysis (equal); Investigation (equal). **Andrea Armaroli:** Conceptualization (equal); Formal analysis (equal); Investigation (equal); Writing – review & editing (equal). **Debbie Eelink:** Formal analysis (equal); Writing – review & editing (equal). **Amin Chabchoub:** Supervision (equal); Writing – review & editing (equal). **Jerome Kasparian:** Funding acquisition (lead); Supervision (equal); Writing – review &

editing (equal). **Maura Brunetti:** Conceptualization (equal); Formal analysis (equal); Investigation (equal); Methodology (lead); Supervision (equal); Writing – original draft (lead); Writing – review & editing (equal).

DATA AVAILABILITY

The data that support the findings of this study and the MATLAB scripts are available from the corresponding author upon reasonable request.

APPENDIX A: DISPERSION AND NONLINEAR COEFFICIENTS

The dispersion coefficients are

$$\hat{\alpha} = \frac{1}{2} \omega''(k_0) = \alpha c_g^3, \tag{A1}$$

$$\alpha = -\frac{1}{2} k''(\omega_0) = -\frac{1}{2\omega_0 c_g} \left[1 - \frac{gh}{c_g^2} (1 - \kappa\sigma)(1 - \sigma^2) \right], \tag{A2}$$

$$\hat{\alpha}_3 = \frac{1}{6} \omega'''(k_0) = \frac{\omega_0}{48k_0^3 \sigma} \left[3\sigma + \kappa(1 - \sigma^2)(-3 + \kappa \times \left(-\frac{3}{\sigma} + \frac{3\kappa}{\sigma^2} + 13\kappa - 15\kappa(1 - \sigma^2) - 9\sigma \right)) \right], \tag{A3}$$

$$\alpha_3 = -\frac{1}{6} k'''(\omega_0) = \frac{\hat{\alpha}_3}{c_g^4} - 2\alpha^2 c_g, \tag{A4}$$

$$k'''(\omega_0) = -\frac{1}{c_g^4} \frac{\partial^2 c_g}{\partial k^2} + \frac{3}{c_g^5} \left(\frac{\partial c_g}{\partial k} \right)^2, \tag{A5}$$

$$\hat{\alpha}_4 \equiv \frac{1}{24} \frac{\partial^4 \omega}{\partial k^4} = \frac{\omega_0}{384k_0^4} \left[-15 + 12\kappa^2 + 46\kappa^4 + 4\kappa(3 - 5\kappa^2) \coth \kappa + 2\kappa^2(3 + 10\kappa^2) \coth^2 \kappa + 12\kappa^3 \coth^3 \kappa - 15\kappa^4 \coth^4 \kappa + \kappa\sigma(-12 + 68\kappa^2 + 3\kappa\sigma(-6 - 52\kappa^2 + 5\kappa\sigma(-4 + 7\kappa\sigma))) \right], \tag{A6}$$

03 November 2023 13:25:55

$$\alpha_4 \equiv \frac{1}{24} \frac{\partial^4 k}{\partial \omega^4} = -\frac{1}{24c_g^5} \frac{\partial^3 c_g}{\partial k^3} + \frac{5}{12c_g^6} \frac{\partial^2 c_g}{\partial k^2} \frac{\partial c_g}{\partial k} - \frac{5}{8c_g^7} \left(\frac{\partial c_g}{\partial k} \right)^3$$

$$= -\frac{\hat{\alpha}_4}{c_g^5} + \frac{5}{c_g^6} \hat{\alpha}_3 \hat{\alpha} - \frac{5}{c_g^7} \hat{\alpha}^3, \tag{A7}$$

where $\kappa = k_0 h$, $\sigma = \tanh \kappa$, and c_g is the group velocity,

$$c_g \equiv \frac{\partial \omega}{\partial k} = \frac{g}{2\omega_0} [\sigma + \kappa(1 - \sigma^2)]. \tag{A8}$$

The third-order nonlinear coefficients are

$$\hat{\beta}_D = -\frac{\omega_0 k_0^2}{16\sigma^4} (2\sigma^6 - 13\sigma^4 + 12\sigma^2 - 9), \tag{A9}$$

$$\hat{\beta} = \beta c_g = \hat{\beta}_D + \omega_0 k_0^2 \frac{\mu_g^2}{8\sigma^2 \nu} = \hat{\beta}_D - \frac{k_0 \mu_g}{4\sigma h} D, \tag{A10}$$

$$\beta_D = \frac{\hat{\beta}_D}{c_g}, \tag{A11}$$

$$\beta = \frac{\omega_0 k_0^2}{16\sigma^4 c_g} \left\{ 9 - 10\sigma^2 + 9\sigma^4 - \frac{2\sigma^2 c_g^2}{gh - c_g^2} \right.$$

$$\left. \times \left[4 \frac{c_p^2}{c_g^2} + 4 \frac{c_p}{c_g} (1 - \sigma^2) + \frac{gh}{c_g^2} (1 - \sigma^2)^2 \right] \right\}, \tag{A12}$$

where, interestingly, the coefficients in the curly brackets can be expressed in terms of κ , $c_g/c_p = (\sigma + \kappa(1 - \sigma^2))/(2\sigma)$, $gh/c_g^2 = (c_p^2/c_g^2)\kappa/\sigma$, $2\sigma^2 c_g^2/(gh - c_g^2) = 2\sigma(c_p^2/c_g^2)/(\kappa/\sigma - c_g^2/c_p^2)$ and

$$D = -h \frac{\omega_0 k_0 \mu_g}{2 \sigma \nu} = \frac{\omega_0 \kappa}{2} \frac{2 + (1 - \sigma^2)c_g/c_p}{\kappa - \sigma c_g^2/c_p^2} = \frac{D'}{1 - c_g^2/(gh)}, \tag{A13}$$

$$D' = \frac{\omega_0}{2\sigma} (1 + C_{FD}), \tag{A14}$$

$$\mu_g = \frac{2\sigma}{\omega_0} (2\omega - kc_g(\sigma^2 - 1)) = (\sigma^2 - 1)^2 \kappa - \sigma(\sigma^2 - 5)$$

$$= 4\sigma(1 + C_{FD}), \tag{A15}$$

$$\nu = \frac{4k_0 \sigma}{g} (c_g^2 - gh) = [(\sigma + 1)^2 \kappa - \sigma][(\sigma - 1)^2 \kappa - \sigma], \tag{A16}$$

$$C_{FD} = \frac{\omega_0 c_g}{g \sinh(2\kappa)}. \tag{A17}$$

The higher-order nonlinear coefficients are

$$\beta_{21} = \frac{\hat{\beta}_{21}}{c_g^2} - 4\alpha\beta c_g, \tag{A18}$$

$$\beta_{22} = \frac{\hat{\beta}_{22}}{c_g^2} - 2\alpha\beta c_g, \tag{A19}$$

$$\hat{\beta}_{21} = \omega_0 k_0 Q_{41S}, \tag{A20}$$

$$\hat{\beta}_{22} = \omega_0 k_0 Q_{42S}, \tag{A21}$$

$$B_{21} = \omega_0 k_0 \tilde{Q}_{41}/c_g^2 - 4\alpha\beta_D c_g, \tag{A22}$$

$$B_{22} = \omega_0 k_0 \tilde{Q}_{42}/c_g^2 - 2\alpha\beta_D c_g, \tag{A23}$$

where Q_{41S} , Q_{42S} , \tilde{Q}_{41} , \tilde{Q}_{42} are given in Appendix B.

APPENDIX B: NOTATION USED IN SEDLETSKY (2003) (SED03)

The main coefficients in Sedletsky's notation are³⁹

$$Q_{41} = \tilde{Q}_{41} - \frac{\mu_g}{\nu} \tilde{q}_{40}, \tag{B1}$$

$$Q_{42} = \tilde{Q}_{42} + \frac{\mu_g}{\nu} \tilde{q}_{40}, \tag{B2}$$

$$\tilde{q}_{40} = \frac{1}{32\sigma^3 \nu} [(\sigma^2 - 1)^5 \kappa^4 - 4\sigma(2\sigma^4 + 9\sigma^2 + 5)(\sigma^2 - 1)^2 \kappa^3$$

$$+ 2\sigma^2(9\sigma^4 + 16\sigma^2 - 9)(\sigma^2 - 1)\kappa^2$$

$$- 4\sigma^3(4\sigma^4 - 9\sigma^2 - 7)\kappa + 5\sigma^4(\sigma^2 - 5)], \tag{B3}$$

$$\tilde{Q}_{41} = \tilde{q}_{41} = \frac{1}{16\sigma^5 \nu} [(2\sigma^6 - 11\sigma^4 - 10\sigma^2 + 27)(\sigma^2 - 1)^3 \kappa^3$$

$$- \sigma(6\sigma^8 - 21\sigma^6 + 9\sigma^4 - 43\sigma^2 + 81)(\sigma^2 - 1)\kappa^2$$

$$+ \sigma^2(6\sigma^8 - 15\sigma^6 - 77\sigma^4 + 71\sigma^2 - 81)\kappa$$

$$- \sigma^3(\sigma^2 + 1)(2\sigma^4 - 7\sigma^2 - 27)], \tag{B4}$$

$$\tilde{q}_{42} = \frac{1}{32\sigma^5 \nu} [(4\sigma^6 - 13\sigma^4 + 10\sigma^2 - 9)(\sigma^2 - 1)^3 \kappa^3$$

$$- \sigma(12\sigma^8 - 51\sigma^6 + 17\sigma^4 - \sigma^2 - 9)(\sigma^2 - 1)\kappa^2$$

$$+ \sigma^2(12\sigma^8 - 67\sigma^6 + 33\sigma^4 - \sigma^2 - 9)\kappa$$

$$- \sigma^3(4\sigma^6 - 29\sigma^4 + 42\sigma^2 - 9)], \tag{B5}$$

$$q_3 = -\frac{\hat{\beta}}{\omega_0 k_0^2}, \tag{B6}$$

$$\tilde{Q}_{42} = \tilde{q}_{42} - 2 \frac{c_g}{c_p} q_3. \tag{B7}$$

The final expressions for Q_{41} and Q_{42} are given in Eqs. (67) and (68) in Ref. 39 and reported here for completeness,

$$Q_{41} = \frac{1}{32\sigma^5 \nu^2} \{ (3\sigma^6 - 20\sigma^4 - 21\sigma^2 + 54)(\sigma^2 - 1)^5 \kappa^5$$

$$- \sigma(11\sigma^8 - 99\sigma^6 - 61\sigma^4 + 7\sigma^2 + 270)(\sigma^2 - 1)^3 \kappa^4$$

$$+ 2\sigma^2(\sigma^2 - 1)(7\sigma^{10} - 58\sigma^8 + 38\sigma^6 + 52\sigma^4 - 181\sigma^2 + 270)\kappa^3$$

$$- 2\sigma^3(3\sigma^{10} + 18\sigma^8 - 146\sigma^6 - 172\sigma^4 + 183\sigma^2 - 270)\kappa^2$$

$$- \sigma^4(\sigma^8 - 109\sigma^6 + 517\sigma^4 + 217\sigma^2 + 270)\kappa$$

$$+ \sigma^5(\sigma^6 - 40\sigma^4 + 193\sigma^2 + 54) \}, \tag{B8}$$

$$Q_{42} = \frac{1}{32\sigma^5 \nu^2} \{ -(3\sigma^6 + 7\sigma^4 - 11\sigma^2 + 9)(\sigma^2 - 1)^5 \kappa^5$$

$$+ \sigma(11\sigma^8 - 48\sigma^6 + 66\sigma^4 + 8\sigma^2 + 27)(\sigma^2 - 1)^3 \kappa^4$$

$$- 2\sigma^2(\sigma^2 - 1)(7\sigma^{10} - 79\sigma^8 + 282\sigma^6 - 154\sigma^4 - \sigma^2 + 9)\kappa^3$$

$$+ 2\sigma^3(3\sigma^{10} - 63\sigma^8 + 314\sigma^6 - 218\sigma^4 + 19\sigma^2 + 9)\kappa^2$$

$$+ \sigma^4(\sigma^8 + 20\sigma^6 - 158\sigma^4 - 28\sigma^2 - 27)\kappa$$

$$- \sigma^5(\sigma^6 - 7\sigma^4 + 7\sigma^2 - 9) \}. \tag{B9}$$

We have verified that they are equivalent to the expressions obtained using Eqs. (B1) and (B2).

From Eqs. (B8) and (B9), in the deep-water limit $\kappa \rightarrow \infty$, $\sigma \rightarrow 1$, $\nu \rightarrow 1 - 4\kappa$, $\mu_g \rightarrow 4$, $Q_{41} \rightarrow 768/(32 \cdot 16) = 3/2$, and $Q_{42} \rightarrow 128/(32 \cdot 16) = 1/4$ recovering the Dysthe result for such terms.

As suggested in Ref. 41, the above-mentioned expressions can be modified to agree with the results presented in Ref. 40. However, we have verified that the (small) modification suggested in Ref. 41 missed a factor 2, the right one being the following:

$$\tilde{q}_{40S} = \tilde{q}_{40} + \frac{\Delta}{2} \frac{\nu}{\mu_g}, \tag{B10}$$

$$Q_{41S} = Q_{41} - \frac{\Delta}{2}, \tag{B11}$$

$$Q_{42S} = Q_{42} + \frac{\Delta}{2}, \tag{B12}$$

where the term Δ is defined in Ref. 41,

$$\begin{aligned} \Delta = & -\frac{\sigma^2 - 1}{16\sigma^3\nu} [(\sigma^2 - 1)^3(3\sigma^2 + 1)\kappa^3 \\ & - \sigma(\sigma^2 - 1)(5\sigma^4 - 18\sigma^2 - 3)\kappa^2 \\ & + \sigma^2(\sigma^2 - 1)(\sigma^2 - 9)\kappa + \sigma^3(\sigma^2 - 5)]. \end{aligned} \tag{B13}$$

In the deep-water limit, $\kappa \rightarrow \infty$, $Q_{41S} \rightarrow 3/2$, and $Q_{42S} \rightarrow 1/4$, since $\Delta \rightarrow 0$, thus recovering the Dysthe result for such terms.

Note, however, that the final equations that include the mean flow [namely, Eqs. (2) and (34)] are not affected by such ambiguity, since their high-order nonlinear coefficients only depend on \tilde{Q}_{41} and \tilde{Q}_{42} .

APPENDIX C: NOTATION USED IN SLUNYAEV (2005) (SLU05)

One can use the notation in Ref. 40, where $\hat{\beta}_{21} = \omega_0 k_0 Q_{41S}$ and $\hat{\beta}_{22} = \omega_0 k_0 Q_{42S}$, and $Q_{41S} = (h^3 \omega_0) \tilde{\alpha}_{21} / (\kappa^3 \sigma^2)$, $Q_{42S} = (h^3 \omega_0) \tilde{\alpha}_{22} / (\kappa^3 \sigma^2)$, with $\tilde{\alpha}_{21} = \tilde{\rho}_{21} - \tilde{\rho}_{12} \gamma_2$ and $\tilde{\alpha}_{22} = \tilde{\rho}_{22} + \tilde{\rho}_{12} \gamma_2$, $\tilde{\rho}_{21} = P_{21} + s \beta_1 \gamma_1$, $\tilde{\rho}_{22} = P_{22} - s \beta_1 \gamma_1$. Here, $\beta_1 = -\hat{\alpha}$ and the other coefficients are given by⁵⁷

$$\begin{aligned} h^3 \omega_0 P_{21} = & \left(\kappa^2 \frac{(\sigma^2 - 1)(-4\sigma^4 + 3\sigma^2 + 1)}{8\sigma^2} \right. \\ & \left. + \kappa \frac{4\sigma^4 - 9\sigma^2 + 3}{4\sigma} + \frac{-4\sigma^2 + 19}{8} \right) h^3 \omega_0 \gamma_1 \\ & + \kappa^2 \frac{-\sigma^4 + 3}{2(\sigma^2 + 1)} h \omega_0 \chi_2 \\ & + \left(\kappa^2 \frac{-3\sigma^6 + 7\sigma^4 - 9\sigma^2 - 3}{4\sigma(\sigma^2 + 1)} + 3\kappa \frac{\sigma^4 - 5}{4(\sigma^2 + 1)} \right) h^2 \omega_0 \chi_1 \\ & + \kappa^4 \frac{(\sigma^2 - 1)(11\sigma^4 - 12\sigma^2 - 3)}{16\sigma} + \kappa^3 \frac{-11\sigma^4 + 40\sigma^2 - 9}{16}, \end{aligned} \tag{C1}$$

$$\begin{aligned} h^3 \omega_0 P_{22} = & \left(-\kappa^2 \frac{(\sigma^2 - 1)^2}{8} + \kappa \frac{\sigma^4 - 5\sigma^2 + 2}{4\sigma} + \frac{-\sigma^2 + 8}{8} \right) h^3 \omega_0 \gamma_1 \\ & + \left(\kappa^2 \frac{(\sigma^2 - 1)(\sigma^4 + 3)}{4\sigma(\sigma^2 + 1)} - \kappa \frac{\sigma^4 + 3}{4(\sigma^2 + 1)} \right) h^2 \omega_0 \chi_1 \\ & + \kappa^4 \frac{(\sigma^2 - 1)(-3\sigma^4 - 8\sigma^2 + 3)}{32\sigma} + 3\kappa^3 \frac{\sigma^4 - 1}{32}, \end{aligned} \tag{C2}$$

$$h^2 \omega_0 s = \kappa^2 \frac{\sigma^2 - 1}{2}, \tag{C3}$$

$$V_d^2 = gh - c_g^2 = -\frac{g\nu}{4k_0\sigma}, \tag{C4}$$

$$h^3 \omega_0 \gamma_1 = h^3 \omega_0 \frac{k_0^2 c_g (\sigma^2 - 1) - 2\omega_0 k_0}{4V_d^2} = \frac{\kappa^3 \sigma \mu_g}{2\nu}, \tag{C5}$$

$$\gamma_2 = \frac{1}{V_d^2} \left[2c_g \gamma_1 \beta_1 + k_0^2 \beta_1 \frac{(\sigma^2 - 1)}{4} + \frac{\omega^2 - k_0^2 c_g^2 (\sigma^2 - 1)}{4\omega_0} \right], \tag{C6}$$

$$\tilde{\rho}_{12} = \frac{2\omega_0 k_0 - k_0^2 c_g (\sigma^2 - 1)}{2\omega_0} = \frac{k \mu_g}{4\sigma}, \tag{C7}$$

$$h^2 \omega_0 \chi_1 = 3\kappa^2 \frac{\sigma^4 - 1}{8\sigma^2}, \tag{C8}$$

$$\begin{aligned} h \omega_0 \chi_2 = & \left(\kappa \frac{-\sigma^3 + 3}{\sigma} + 1 \right) \frac{h^2 \omega_0 \chi_1}{\kappa} + \frac{3\kappa^2 (\sigma^2 - 1)(3\sigma^2 + 1)}{16\sigma} \\ & + 9\kappa \frac{1 - \sigma^4}{16\sigma^2}. \end{aligned} \tag{C9}$$

Using the same notation as in Sed03 for the reconstruction at leading order of the surface elevation, $\eta(\chi, t) = \frac{1}{2}[U(x, t) \exp(i(k_0 \chi - \omega_0 t)) + c.c.]$, the mean flow term is written as [see Eqs. (32), (43), and (45) in Ref. 40]

$$\frac{\partial \phi_0}{\partial x} = \frac{\omega_0 k_0 \mu_g}{2 \sigma \nu} |U|^2 - i \frac{c_p^2}{\sigma^2} \left(\gamma_2 + \frac{\beta_1 \gamma_1}{c_g} \right) \left(U \frac{\partial U^*}{\partial x} - U^* \frac{\partial U}{\partial x} \right). \tag{C10}$$

Note that while the first term is equal to the corresponding term in Eq. (3) from Sedletsky's derivation, the second one has a different coefficient, since $4\omega_0 \sigma \tilde{q}_{40} / \nu \neq c_p^2 \sigma^2 (\gamma_2 + \beta_1 \gamma_1 / c_g) / \sigma^2$ [even if we take into account the correction \tilde{q}_{40S} in Eq. (B10)].

Using Eq. (33), the derivative in time of ϕ_0 is

$$\frac{\partial \phi_0}{\partial t} = -c_g \frac{\omega_0 k_0 \mu_g}{2 \sigma \nu} |U|^2 - i \frac{c_p^2}{\sigma^2} \left(\gamma_2 + \frac{\beta_1 \gamma_1}{c_g} \right) \left(U \frac{\partial U^*}{\partial t} - U^* \frac{\partial U}{\partial t} \right). \tag{C11}$$

APPENDIX D: EXAMPLE OF SEA STATE REALIZATION

Following the definitions in Ref. 51, we consider a Gaussian amplitude spectrum, denoted by $S(k)$, given by

$$S(k) = \exp \left(-\frac{(k - k_0)^2}{2k_w^2} \right), \tag{D1}$$

for $k > 0$, where $k_0 = 0.0277 \text{ m}^{-1}$, and $k_w = 0.27 k_0$ is the dimensional bandwidth. Other spectra, like JONSWAP or Pierson–Moskowitz, can also be used. This yields the following surface elevation at first order in steepness:

$$\eta_1(x, t) = \frac{A_p}{2} \frac{\int_0^\infty S(k) e^{i[k(x-x_f) - \omega(t-t_f)]} dk}{\int_0^\infty S(k) dk} + c.c., \tag{D2}$$

where A_p , x_f , and t_f are the amplitude, position, and time for the group at linear focus, with steepness given by $\epsilon = A_p k_0 = 0.3$. An example of sea state realization at second order in steepness,

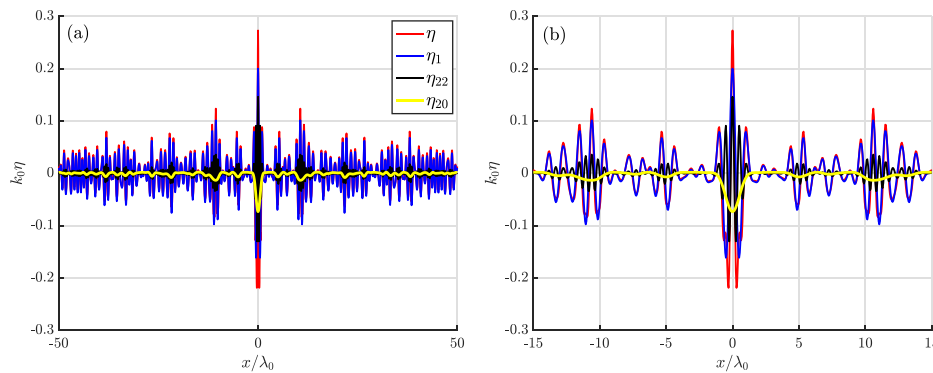


FIG. 9. Sea surface elevation η and its components at first (η_1) and second order in steepness (η_{22} and the set-down η_{20}) in the case of a focused wave group at the origin for $k_0h = 1.5$: (a) full range of considered spatial values and (b) the same as (a), zoomed on $30\lambda_0$.

obtained using the Dalzell development,⁵⁰ is shown in Fig. 9 for the case of a focused wave group at $x_f=0$, $t_f=0$ for $k_0h = 1.5$. The power spectrum can be obtained as⁵⁸ $P(k) = |\hat{\eta}|^2 / (2dk)$, where $\hat{\eta}$ is the Fourier transform in space of the surface elevation, from which the significant wave height H_s can be obtained as $H_s = 4\sqrt{m_0} = 5.2$ m, m_0 being equal to the area under the power spectrum curve.

REFERENCES

- G. G. Stokes, "On the theory of oscillatory waves," *Trans. Cam. Philos. Soc.* **8**, 441–455 (1847).
- T. S. van den Bremer and Ø. Breivik, "Stokes drift," *Philos. Trans. R. Soc. A* **376**, 20170104 (2018).
- M. Bjørnstad, M. Buckley, H. Kalisch, M. Streßer, J. Horstmann, H. G. Frøysa, O. E. Ige, M. Cysewski, and R. Carrasco-Alvarez, "Lagrangian measurements of orbital velocities in the surf zone," *Geophys. Res. Lett.* **48**, e2021GL095722, <https://doi.org/10.1029/2021GL095722> (2021).
- R. Calvert, C. Whittaker, A. Raby, P. H. Taylor, A. G. L. Borthwick, and T. S. van den Bremer, "Laboratory study of the wave-induced mean flow and set-down in unidirectional surface gravity wave packets on finite water depth," *Phys. Rev. Fluids* **4**, 114801 (2019).
- J. D. Carter, C. W. Curtis, and H. Kalisch, "Particle trajectories in nonlinear Schrödinger models," *Water Waves* **2**, 31–57 (2020).
- M. H. DiBenedetto, "Non-breaking wave effects on buoyant particle distributions," *Front. Mar. Sci.* **7**, 148 (2020).
- A. Cózar, F. Echevarría, J. I. González-Gordillo, X. Irigoien, B. Úbeda, S. Hernández-León, A. T. Palma, S. Navarro, J. G. de Lomas, A. Ruiz, M. L. F. de Puellas, and C. M. Duarte, "Plastic debris in the open ocean," *Proc. Nat. Acad. Sci. U. S. A.* **111**, 10239–10244 (2014).
- K. H. Christensen, Ø. Breivik, K.-F. Dagestad, J. Röhrs, and B. Ward, "Short-term predictions of oceanic drift," *Oceanography* **31**, 59–67 (2018).
- A. V. Babanin, "On a wave-induced turbulence and a wave-mixed upper ocean layer," *Geophys. Res. Lett.* **33**, L20605, <https://doi.org/10.1029/2006GL027308> (2006).
- V. Onink, D. Wichmann, P. Delandmeter, and E. van Sebille, "The role of Ekman currents, geostrophy, and Stokes drift in the accumulation of floating microplastic," *J. Geophys. Res.* **124**, 1474–1490, <https://doi.org/10.1029/2018JC014547> (2019).
- E. van Sebille, S. Aliani, K. L. Law, N. Maximenko, J. M. Alsina, A. Bagaev, M. Bergmann, B. Chapron, I. Chubarenko, A. Cózar, P. Delandmeter, M. Egger, B. Fox-Kemper, S. P. Garaba, L. Goddijn-Murphy, B. D. Hardesty, M. J. Hoffman, A. Isobe, C. E. Jongedijk, M. L. A. Kaandorp, L. Khatmullina, A. A. Koelmans, T. Kukulka, C. Laufkötter, L. Lebreton, D. Lobelle, C. Maes, V. Martinez-Vicente, M. A. M. Maqueda, M. Poulain-Zarcos, E. Rodríguez, P. G. Ryan, A. L. Shanks, W. J. Shim, G. Suaria, M. Thiel, T. S. van den Bremer, and D. Wichmann, "The physical oceanography of the transport of floating marine debris," *Environ. Res. Lett.* **15**, 023003 (2020).
- H. J. Cunningham, C. Higgins, and T. S. van den Bremer, "The role of the unsteady surface wave-driven Ekman–Stokes flow in the accumulation of floating marine litter," *J. Geophys. Res.* **127**, e2021JC018106, <https://doi.org/10.1029/2021JC018106> (2022).
- M. Longuet-Higgins and R. Stewart, "Radiation stresses in water waves; A physical discussion, with applications," *Deep Sea Res. Oceanogr. Abstr.* **11**, 529–562 (1964).
- T. T. Janssen, J. A. Battjes, and A. R. van Dongeren, "Long waves induced by short-wave groups over a sloping bottom," *J. Geophys. Res.* **108**, 3252, <https://doi.org/10.1029/2002JC001515> (2003).
- J. A. Battjes, H. J. Bakkenes, T. T. Janssen, and A. R. van Dongeren, "Shoaling of subharmonic gravity waves," *J. Geophys. Res.* **109**, C02009, <https://doi.org/10.1029/2003JC001863> (2004).
- S. G. Monismith, E. A. Cowen, H. M. Nepf, J. Magnaudet, and L. Thais, "Laboratory observations of mean flows under surface gravity waves," *J. Fluid Mech.* **573**, 131–147 (2007).
- C. W. Curtis, J. D. Carter, and H. Kalisch, "Particle paths in nonlinear Schrödinger models in the presence of linear shear currents," *J. Fluid Mech.* **855**, 322–350 (2018).
- D. J. Benney and G. J. Roskes, "Wave instabilities," *Stud. Appl. Math.* **48**, 377–385 (1969).
- H. Hasimoto and H. Ono, "Nonlinear modulation of gravity waves," *J. Phys. Soc. Jpn.* **33**, 805–811 (1972).
- A. Davey and K. Stewartson, "On three-dimensional packets of surface waves," *Proc. R. Soc. Lond. A* **338**, 101–110 (1974).
- C. C. Mei, M. A. Stiassnie, and D. K.-P. Yue, *Theory and Applications of Ocean Surface Waves* (World Scientific, 2005).
- V. E. Zakharov, "Stability of periodic waves of finite amplitude on the surface of a deep fluid," *J. Appl. Mech. Tech. Phys.* **9**, 190–194 (1972).
- P. A. Janssen and M. Onorato, "The intermediate water depth limit of the Zakharov equation and consequences for wave prediction," *J. Phys. Oceanogr.* **37**, 2389–2400 (2007).
- K. B. Dysthe, "Note on a modification to the nonlinear Schrödinger equation for application to deep water waves," *Proc. R. Soc. Lond. A* **369**, 105–114 (1979).
- A. Chabchoub, N. Hoffmann, M. Onorato, G. Genty, J. M. Dudley, and N. Akhmediev, "Hydrodynamic supercontinuum," *Phys. Rev. Lett.* **111**, 054104 (2013).
- K. Trulsen and C. T. Stansberg, "Spatial evolution of water surface waves: Numerical simulation and experiment of bichromatic waves," in *The Eleventh International Offshore and Polar Engineering Conference* (OnePetro, 2001), pp. 71–77.
- L. Shemer, A. Sergeeva, and A. Slunyaev, "Applicability of envelope model equations for simulation of narrow-spectrum unidirectional random wave field evolution: Experimental validation," *Phys. Fluids* **22**, 016601 (2010).
- A. Goulet and W. Choi, "A numerical and experimental study on the nonlinear evolution of long-crested irregular waves," *Phys. Fluids* **23**, 016601 (2011).
- H. Zhang, C. Guedes Soares, and M. Onorato, "Modelling of the spatial evolution of extreme laboratory wave heights with the nonlinear Schrödinger and Dysthe equations," *Ocean Eng.* **89**, 1–9 (2014).
- A. Armaroli, M. Brunetti, and J. Kasparian, "Recurrence in the high-order nonlinear Schrödinger equation: A low-dimensional analysis," *Phys. Rev. E* **96**, 012222 (2017).

- ³¹A. Slunyaev, E. Pelinovsky, A. Sergeeva, A. Chabchoub, N. Hoffmann, M. Onorato, and N. Akhmediev, "Super-rogue waves in simulations based on weakly nonlinear and fully nonlinear hydrodynamic equations," *Phys. Rev. E* **88**, 012909 (2013).
- ³²P. A. E. M. Janssen, "On a fourth-order envelope equation for deep-water waves," *J. Fluid Mech.* **126**, 1–11 (1983).
- ³³U. Brinch-Nielsen and I. Jonsson, "Fourth order evolution equations and stability analysis for stokes waves on arbitrary water depth," *Wave Motion* **8**, 455–472 (1986).
- ³⁴K. Trulsen and K. B. Dysthe, "A modified nonlinear Schrödinger equation for broader bandwidth gravity waves on deep water," *Wave Motion* **24**, 281–289 (1996).
- ³⁵M. Stiassnie, "Note on the modified nonlinear Schrödinger equation for deep water waves," *Wave Motion* **6**, 431–433 (1984).
- ³⁶S. Debsarma and K. P. Das, "A higher-order nonlinear evolution equation for broader bandwidth gravity waves in deep water," *Phys. Fluids* **17**, 104101 (2005).
- ³⁷O. Gramstad and K. Trulsen, "Hamiltonian form of the modified nonlinear Schrödinger equation for gravity waves on arbitrary depth," *J. Fluid Mech.* **670**, 404–426 (2011).
- ³⁸O. Gramstad, "The zakharov equation with separate mean flow and mean surface," *J. Fluid Mech.* **740**, 254–277 (2014).
- ³⁹Y. V. Sedletsky, "The fourth-order nonlinear Schrödinger equation for the envelope of stokes waves on the surface of a finite-depth fluid," *J. Exp. Theor. Phys.* **97**, 180–193 (2003).
- ⁴⁰A. V. Slunyaev, "A high-order nonlinear envelope equation for gravity waves in finite-depth water," *J. Exp. Theor. Phys.* **101**, 926–941 (2005).
- ⁴¹I. S. Gandzha, Y. V. Sedletsky, and D. S. Dutykh, "High-order nonlinear Schrödinger equation for the envelope of slowly modulated gravity waves on the surface of finite-depth fluid and its quasi-soliton solutions," *Ukr. J. Phys.* **59**, 1201–1215 (2014).
- ⁴²Note that Slu05 uses the opposite convention, giving rise to different signs in some terms with respect to Sed03.
- ⁴³D. H. Peregrine, "Water waves, nonlinear Schrödinger equations and their solutions," *J. Austral. Math. Soc. Ser. B* **25**, 16–43 (1983).
- ⁴⁴E. Lo and C. C. Mei, "A numerical study of water-wave modulation based on a higher-order nonlinear Schrödinger equation," *J. Fluid Mech.* **150**, 395–416 (1985).
- ⁴⁵K. Trulsen and K. B. Dysthe, "Frequency downshift in three-dimensional wave trains in a deep basin," *J. Fluid Mech.* **352**, 359–373 (1997).
- ⁴⁶E. Kit and L. Shemer, "Spatial versions of the zakharov and dysthe evolution equations for deep-water gravity waves," *J. Fluid Mech.* **450**, 201–205 (2002).
- ⁴⁷M. Onorato, A. R. Osborne, M. Serio, and L. Cavaleri, "Modulational instability and non-gaussian statistics in experimental random water-wave trains," *Phys. Fluids* **17**, 078101 (2005).
- ⁴⁸D. Eeltink, A. Lemoine, H. Branger, O. Kimmoun, C. Kharif, J. D. Carter, A. Chabchoub, M. Brunetti, and J. Kasparian, "Spectral up- and downshifting of akhmediev breathers under wind forcing," *Phys. Fluids* **29**, 107103 (2017).
- ⁴⁹A. I. Dyachenko, D. I. Kachulin, and V. E. Zakharov, "Super compact equation for water waves," *J. Fluid Mech.* **828**, 661–679 (2017).
- ⁵⁰J. Dalzell, "A note on finite depth second-order wave-wave interactions," *Appl. Ocean Res.* **21**, 105–111 (1999).
- ⁵¹Y. Li and X. Li, "Weakly nonlinear broadband and multi-directional surface waves on an arbitrary depth: A framework, stokes drift, and particle trajectories," *Phys. Fluids* **33**, 076609 (2021).
- ⁵²J. Orszaghova, P. H. Taylor, A. G. Borthwick, and A. C. Raby, "Importance of second-order wave generation for focused wave group run-up and over-topping," *Coastal Eng.* **94**, 63–79 (2014).
- ⁵³Rahman, M. "Fundamentals concerning Stokes waves," *WIT Trans. Eng. Sci.* **9**, 289 (1996).
- ⁵⁴In particular, the fourth-order dispersion term $\alpha_4 \partial^4 U / \partial t^4$ [to be added on the rhs of Eq. (32)] is generally used to cancel out resonances that can make the model numerically unstable, as discussed in T. Hara and C. C. Mei, "Frequency downshift in narrowbanded surface waves under the influence of wind," *J. Fluid Mech.* **230**, 429–477 (1991).
- ⁵⁵K. Trulsen, I. Kliakhandler, K. B. Dysthe, and M. G. Velarde, "On weakly nonlinear modulation of waves on deep water," *Phys. Fluids* **12**, 2432–2437 (2000).
- ⁵⁶D. Eeltink, A. Armaroli, Y. M. Ducimetière, J. Kasparian, and M. Brunetti, "Single-spectrum prediction of kurtosis of water waves in a nonconservative model," *Phys. Rev. E* **100**, 013102 (2019).
- ⁵⁷We have expressed Slunyaev's coefficients in terms of Sedletsky's expressions defined in *Appendices A* and *B* whenever possible.
- ⁵⁸I. Young, "Wind-generated waves," in *Ocean Wave Dynamics*, edited by I. Young and A. V. Babanin (World Scientific Publishing, Singapore, 2020), Chap. 1, pp. 1–21.